

Nanozymatic Activity of UiO-66 Metal-Organic Frameworks: Tuning the Nanopore Environment Enhances Hydrolytic Activity toward Peptide Bonds

Hong Giang T. Ly,^{[a][b]} Guangxia Fu,^[c] Francisco de Azambuja,^[a] Dirk De Vos,^[c] and Tatjana N. Parac-Vogt*^[a]

^[a] Laboratory of Bioinorganic Chemistry, Department of Chemistry, KU Leuven, Celestijnenlaan 200F, 3001 Leuven, Belgium

^[b] Department of Chemistry, College of Natural Sciences, Can Tho University, Can Tho, Vietnam

^[c] Centre for Membrane Separations, Adsorption, Catalysis and Spectroscopy for Sustainable Solutions (cMACS), KU Leuven, Celestijnenlaan 200F, 3001 Leuven, Belgium

ABSTRACT

Proteolytic activity of heterogeneous Zr-based nanozymes is a promising technology for the development of selective protein cleavage protocols which are pivotal in modern proteomics. Here, we report the hydrolytic activity of nanoporous Zr₆-based UiO-66 metal-organic framework (MOF) toward peptide bonds in a series of peptides and in hen egg white lysozyme protein. The standard UiO-66 MOF featuring unsubstituted 1,4-benzenedicarboxylate linkers hydrolyzed the glycyglycine with a rate constant of $7.9 \times 10^{-7} \text{ s}^{-1}$, ($t_{1/2} = 10$ days), which represents $>10^4$ -fold acceleration compared to the uncatalyzed reaction. Further, this reactivity was compared with UiO-66 analogs synthesized using modified linkers bearing NO₂ and NH₂ substituents, or using trifluoroacetic acid as a modulator. Although the overall crystalline structure and particle size of these UiO-66 derivatives were generally conserved, they presented distinct nanoporous structures that could be directly correlated with the reaction rates at least an order of magnitude faster than the parent UiO-66 MOF. Further, the modified nanoporous structures also provided distinct reactivities across a series of dipeptide substrates probed. We propose that these differences might arise from the distinct MOF Lewis and Brønsted acidity resulting from the structural modifications. These findings highlight the potential of further optimizing Zr₆-based MOF nanozymes to achieve residue-selective hydrolytic activity.

Keywords: Metal-organic framework, UiO-66, hydrolysis, peptide bond, artificial proteases, heterogeneous catalysis, nanozymes

INTRODUCTION

Protein digestion technology is of paramount importance in chemical biology, proteomics and therapeutics applications.¹⁻³ Given the large sizes and structural complexity of proteins, methods of digestion that are site-selective are preferred because they largely facilitate data processing and interpretation.⁴ To date, proteolytic enzymes (e.g., trypsin) are by far the method-of-choice to digest proteins selectively in a short time.⁵ However, their narrow stability window, high cost and difficult recoverability limits their wide application. Moreover, trypsin catalyzed protein hydrolysis results only in small fragments, thereby limiting the proteomic information that can be retrieved from the original structure.⁶⁻⁷

Catalytic nanomaterials have been attracting increasing attention over the last decades as potential artificial enzymes. Compared to natural enzymes, they have lower cost, higher stability towards a wide range of conditions, and much easier recyclability, among other advantages.⁸⁻¹⁰ In addition, the rapid evolution in the synthesis of nanomaterials allows better control of their specific molecular and morphological characteristics, which renders them as promising artificial surrogates for the natural enzymes. To date, although many nanomaterials have been described as potential nanozymes, very few have been reported to possess hydrolase or protease activity.⁹ Given the current central role of selective protein hydrolysis in many areas of bioscience, the study and development of proteolytic nanomaterials (nano proteases) is highly desired.

Heterogeneous metal-oxo cluster (MOC) based nanozymes have recently emerged as valuable alternatives towards efficient artificial proteases.¹¹⁻¹⁴ Traditionally, peptide bond hydrolysis in peptides, oligopeptides and proteins has been achieved by using Lewis acidic metal complexes.¹⁵⁻¹⁶ Our contribution to the field concerns the discovery and development of MOCs unique potential as robust and selective catalysts to cleave the peptide bond. At first, we explored water soluble metal-substituted polyoxometalates (POMs),¹⁷⁻²¹ and demonstrated their potential as highly selective proteases.²²⁻²⁹ However, the practical applications of POMs were largely hampered by their difficult separation from proteins. Thus, we recently turned our attention to heterogeneous MOC-based nanomaterials, aiming to expedite catalyst and protein digest separation while keeping the selectivity hallmark of our initial studies. Such effort already resulted in the discovery of new heterogeneous artificial nanoproteases, which include the MOF-808,¹² NU-1000¹³ and the discrete Hf oxo-cluster $[\text{Hf}_{18}\text{O}_{10}(\text{OH})_{26}(\text{SO}_4)_{13}(\text{H}_2\text{O})_{33}]$.¹⁴ Despite their highly promising proteolytic activity, very little is known about the structure-activity relationship of these emerging nano proteases. Furthermore, the catalytic efficiencies of nanozymes are not yet comparable to the natural enzymes, and further studies of their structure-activity relationship are therefore necessary to enable future practical applications.

Metal-organic frameworks (MOFs) are highly tailorable hybrid nanomaterials featuring metal ions or clusters interconnected by organic linkers.³⁰ Their nanoscale porosity, high surface area, good thermal stability and uniformly structured cavities containing catalytically active sites³¹ hold great

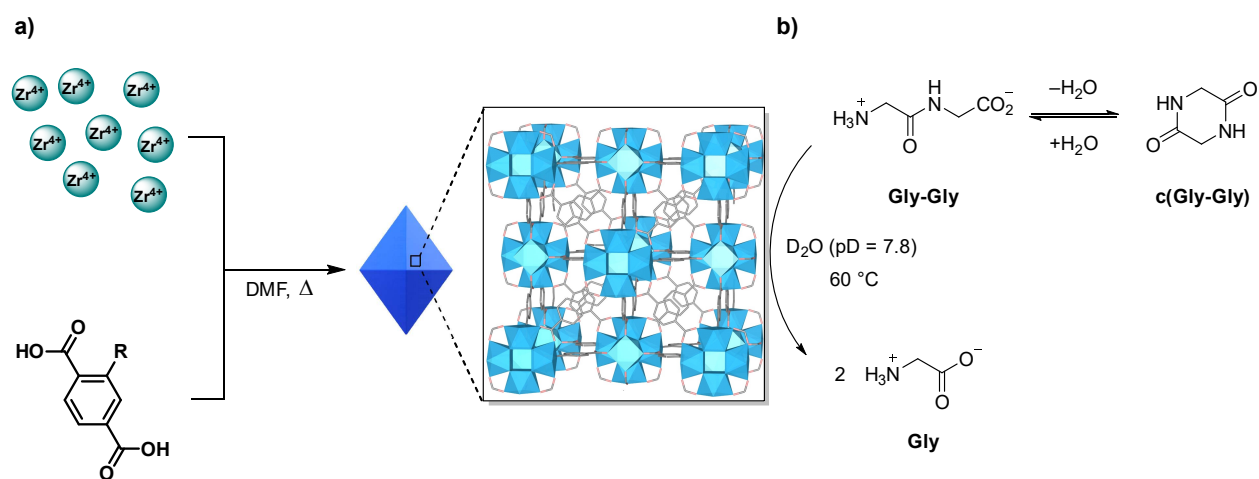
potential for a broad range of applications such as gas storage and separation,³² detection and decomposition of warfare agents,³³ drug delivery³⁴ and (bioinspired)³⁵ catalysis.³⁶⁻³⁸ Among the several MOFs available, Zr-based UiO-66 MOFs is one of the most well-established and versatile structures for probing the impact of surgical structural changes on the reactivity.³⁹ In the past, we have used UiO-66 as a prototype MOF to demonstrate the effect of ligand electronics⁴⁰ and the use of trifluoroacetic acid as a synthetic modulator⁴¹ on the reactivity. Such approach allowed us to tune the Lewis acidity of Zr₆-clusters and the availability of coordinatively unsaturated Zr sites which are presumed catalytic sites without impacting the overall MOF architecture.⁴²

Given the success of this approach, we envisioned the same system could offer valuable insights towards the optimization of emergent and highly promising protease activity of Zr₆-based MOF nanozymes. Therefore, we set out investigate the peptidase activity of UiO-66 in model dipeptides and compare it to three representative analogs prepared with electro-rich or electron-deficient ligands, or in the presence of trifluoroacetic acid as a synthesis modulator. Using the standard UiO-66, we also showcase the selective protease activity of UiO-66 MOF architecture.

RESULTS AND DISCUSSION

UiO-66 hydrolytic activity in model peptide and protein substrates

Following our previous studies, we initially characterized the reactivity of conventional UiO-66 (Scheme 1a) using the hydrolysis of glycyglycine (GlyGly) at 60 °C and pD 7.8 as a model system (Scheme 1b).^{12, 43} As expected, following the reaction by ¹H NMR over time revealed an overall hydrolysis of Gly-Gly to glycine, and the transient formation of cyclic Gly-Gly (c(Gly-Gly)) in small amount in the first hours of reaction (Figure 1a, Figure S4). Fitting the conversion of Gly-Gly to a pseudo-first order kinetics model afforded a rate constant of $7.9 \times 10^{-7} \text{ s}^{-1}$, corresponding to a half-life ($t_{1/2}$) of 10 days (Figure 1b). Comparing these parameters with the estimated 350 years half-life of the uncatalyzed reaction under physiological pH and 60 °C clearly evidences the potential of UiO-66 in catalyzing the peptide bond cleavage.⁴⁴ Besides, a standard filtration test supported the heterogeneous nature of the reaction (Figure S8a), and promising recyclability was showcased washing the recovered UiO-66 with water and methanol before drying and re-activation. While stable in the first two cycles, the catalytic activity dropped ~10% in the third run (Figure S9a), even though Powder X-Ray Diffraction (PXRD) pattern (Figure S10a) and FT-IR (Figure S11) analysis evidenced the overall crystallinity remained stable after three cycles.



Scheme 1. (a) Synthesis of UiO-66 MOFs and its nanoporous crystalline structure (see also Table 1); (b) Nanozymatic peptidase activity of UiO-66 MOFs was developed using the hydrolysis of Gly-Gly as a model reaction.

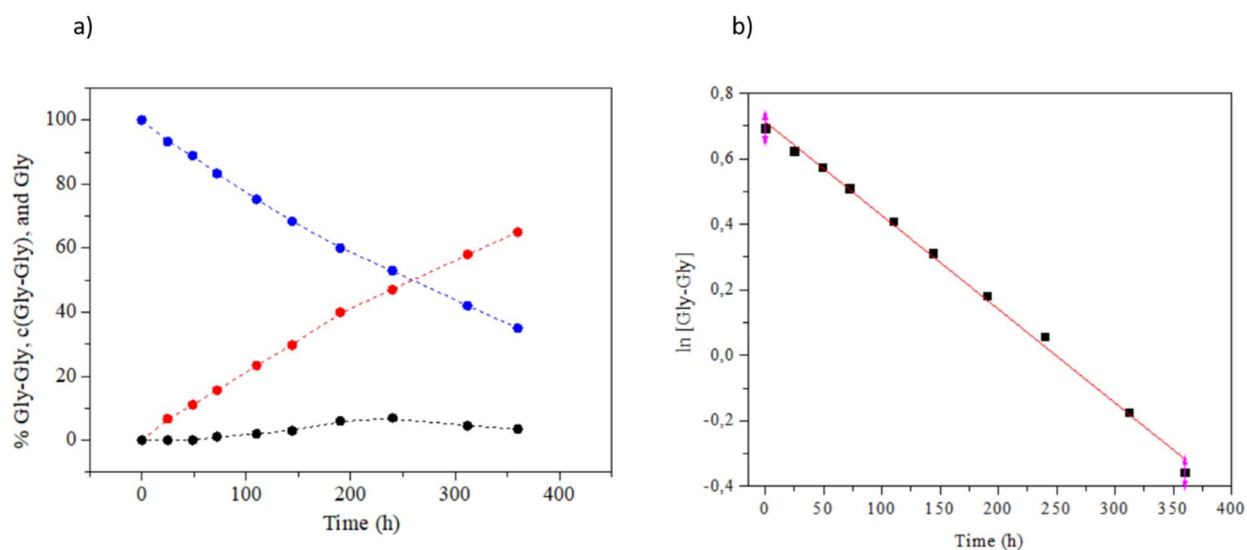


Figure 1. (a) Percentage of Gly-Gly (blue), c(Gly-Gly) (black), and Gly (red) as a function of time (b) $\ln[\text{Gly-Gly}]$ as a function of time for the hydrolysis of 2.0 μmol of Gly-Gly by 2.0 μmol of UiO-66 at pD 7.8 and 60 °C.

Reactivity of UiO-66 was further tested toward the hydrolysis of hen egg white lysozyme protein (HEWL), a 14.3 kDa globular protein containing 129 amino acids. HEWL and UiO-66 were incubated at 60 °C and pH 7.4 in water, as the MOF was not stable in phosphate buffer solution (Figure S12 and S13). The progress of HEWL hydrolysis was followed by SDS-PAGE (Figure 2). Appearance of five new bands with Mw of ca. 12, 10.5, 9, 6.5 and 4 kDa indicated HEWL was selectively hydrolyzed in the presence of UiO-66. The molecular weights of these bands are similar to those observed before with MOF-808 and NU-1000, and suggests an Asp-selective cleavage

governed by the Zr_6 cluster is likely happening also in this case.¹²⁻¹³ Additional experiments showed no hydrolysis in the absence of MOF (Figure S14), and a faster cleavage with increasing amounts of UiO-66 further attested the catalytic role of UiO-66 in the hydrolysis of HEWL. The disappearance of intact protein band without increasing the intensity of fragments is consistent with a significant adsorption of proteins we have observed in our previous works. Finally, MOF stability under the reaction conditions was confirmed by FT-IR and PXRD analysis of a UiO-66 sample recovered after 3 days of reaction.

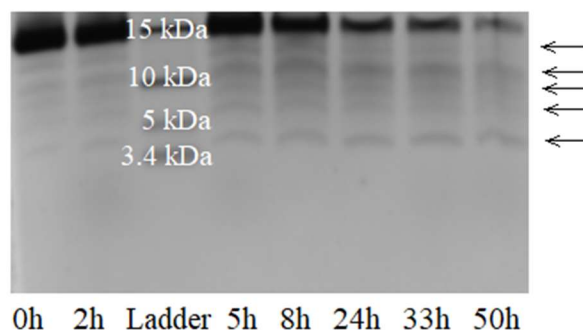


Figure 2. SDS-PAGE gel analysis of HEWL hydrolysis in the presence of UiO-66 in water at 60 °C and pH 7.4 .

Structural change vs. Reactivity for UiO-66 derivatives

Effect of linker electronics. Given the above demonstrated peptidase activity of UiO-66 towards small peptides and proteins, we moved to probe how specific structural changes to the MOF structure would impact the catalytic activity. Inspired by our previous work,⁴⁰ we initially evaluated the impact of electron-withdrawing and electron-donating substituted linkers in hydrolytic activity by preparing UiO-66 analogues using 2-amino- and 2-nitro-1,4-benzenedicarboxylic acids as organic linkers (herein UiO-66-NH₂ and UiO-66-NO₂, respectively, Table 1).⁴⁵ Previously, these UiO-66 variants have provided respectively the slowest and the fastest citronellal cyclization rates relative to regular UiO-66, putatively because of their electronic influence in the Lewis acidity of the Zr_6 node. Therefore, we have chosen these as representative examples seeking to observe opposite influence in the reactivity. Comparison of PXRD patterns (Figure S3) and scanning electron microscopy (SEM) (Figure 3) for both UiO-66 analogues with standard UiO-66 confirmed the overall 3D architecture was preserved for all three MOFs, and the particle size was similar (~200 – 300 nm) in all cases.⁴⁰

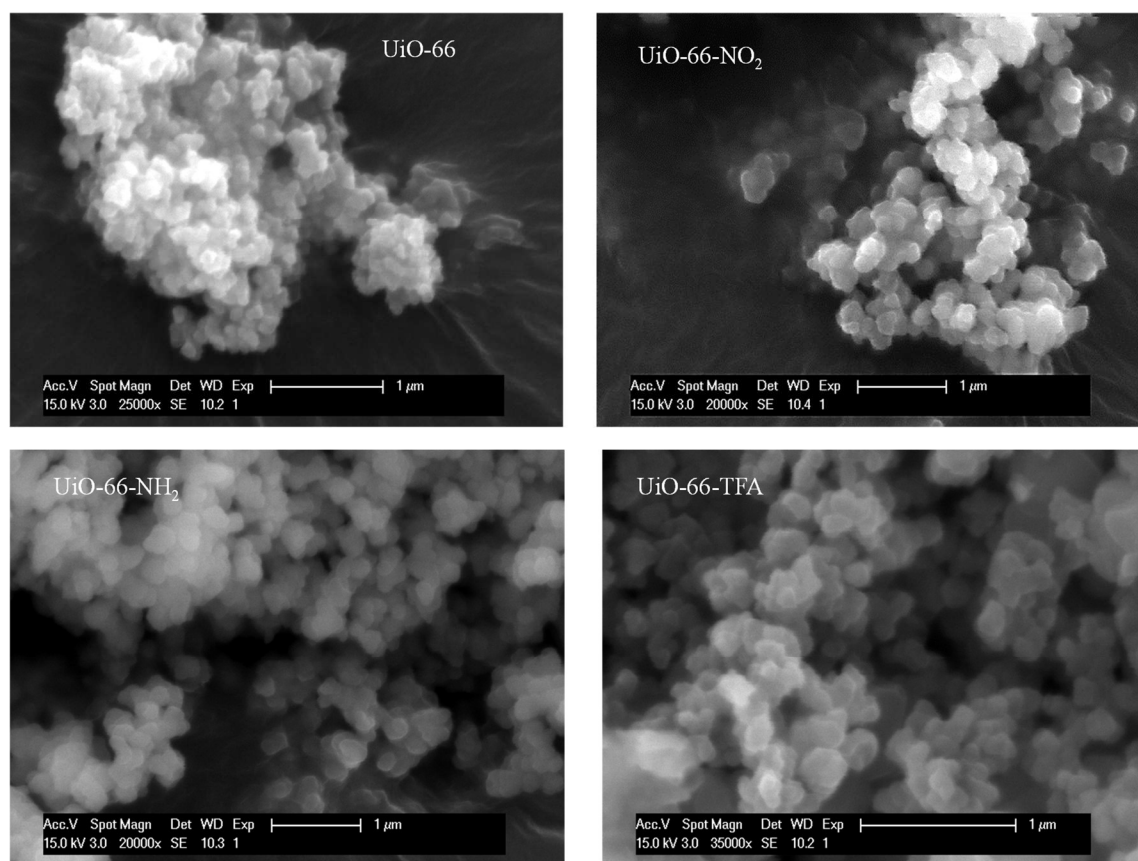
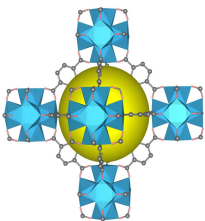
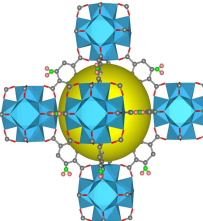
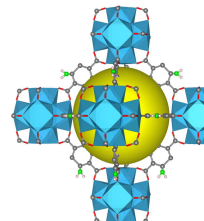
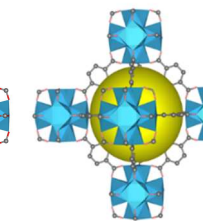


Figure 3: Scanning electron microscopy (SEM) images of as-synthesized UiO-66 MOFs (particle size is around 200nm – 300nm for all the samples).

Both UiO-66-NH₂ or UiO-66-NO₂ hydrolyzed the Gly-Gly faster than the regular UiO-66, but they unexpectedly provided similar reaction rates. While UiO-66-NO₂ hydrolyzed Gly-Gly with a rate constant of $83.6 \times 10^{-7} \text{ s}^{-1}$ ($t_{1/2} = 23 \text{ h}$), the rate constant measured for UiO-66-NH₂ was $89.7 \times 10^{-7} \text{ (s}^{-1})$ ($t_{1/2} = 21.5 \text{ h}$) (Figures S5 and S6). Both mean a *ca.*10-fold increase in the reaction rate compared to standard UiO-66 ($k_{obs} = 7.9 \times 10^{-7} \text{ s}^{-1}$; $t_{1/2} = 240 \text{ h}$). This behavior is surprising because the electron-donating ability of the amino group has been reported to decrease the Lewis acidity of the Zr₆ node,⁴⁰ which in turn would decrease the peptide bond polarization and subsequent susceptibility to a water attack. Therefore, given that particle size was similar among the MOFs tested, we performed a more detailed characterization of the MOFs by nitrogen physisorption isotherms (N₂ isotherms) and thermogravimetric analysis (TGA) to understand the potential reasons behind these unexpected results, especially with regard to the high reactivity of UiO-66-NH₂.⁴⁶

Table 1. Structural features and reactivity of standard UiO-66 MOFs used in this study.

MOF	UiO-66	UiO-66-NO ₂	UiO-66-NH ₂	UiO-66-TFA ⁽¹⁾
Structure				
Linker				
Linkers coordinated/ Zr ₆ cluster ⁽²⁾	8	9	7	7
BET surface area (m ² /g)	861	570	937	985
Particle size (nm)	200 – 300 nm for all UiO-66 MOFs			
t _{1/2} ⁽³⁾	10 days	23 h	21.5	24.2 h
10 ⁷ × k _{obs} (s ⁻¹) ⁽³⁾	7.9	83.6	89.7	79.7

⁽¹⁾ Using trifluoroacetic acid as modulator (see ref. ⁴¹). ⁽²⁾ Linker coordination/Zr₆ cluster estimated from TGA curves as in reference ⁴⁷. ⁽³⁾ Reaction condition: pD = 7.8, 60°C (see main text for details). Color code: Zr₆-cluster: Cyan-blue; C: Grey; N: Green; O: Red; F:blue.

TGA, N₂ isotherms and specific surface areas calculated thereof (BET method) evidenced the UiO-66-NH₂ greater porosity, which is coherent with the higher than expected reactivity observed for this MOF (Table 1). To compare the porosity of standard UiO-66 MOFs and analogues, N₂ physisorption isotherm were collected (Figure S1a), and specific surface areas of the studied MOFs were calculated by the BET method (Table 1 and S1). UiO-66-NH₂ showed the highest BET surface area (937 m²/g), followed by standard UiO-66 (861 m²/g), and UiO-66-NO₂ (570 m²/g) (Table 1). Accordingly, UiO-66-NH₂ also exhibited the largest pore width (14 – 20 Å) (Figure S1b),⁴⁸ and the lowest average number of linkers coordinated per Zr₆ node (Table 1), as indicated by lower linker derived weight loss of UiO-66-NH₂ in the TGA results (Figure S2).⁴⁷ Together, these data clearly indicate that more free catalytic sites are present in UiO-66-NH₂, suggesting its comparable hydrolytic activity derives mainly from its defects. In addition, the larger surface area and pore size of UiO-66-NH₂ could also promote the reactivity by providing easier access of the substrate to the Zr defective sites. Therefore, more defective Zr sites combined with larger pore size resulted in higher catalytic activity compared to UiO-66. Nonetheless, present data does not rule a potential beneficial H-bonding interaction between the substrate and the linker's amino group

as previously described for an aldol reaction.⁴⁹ Together, this data also suggest the added steric hindrance of the NH₂/NO₂ groups nearby the active sites, which could hinder substrates to reach free Zr sites does not have pronounced effect on the reactivity. More interestingly, these data also showcase the strong effect of the NO₂ group in the reactivity, which overrules the lowest number of free catalytic sites and surface area of UiO-66-NO₂ and keeps its hydrolytic activity comparable to the more defective UiO-66-NH₂. Notably, these results indicate that both increasing the number of defects or using the linker electronics can in principle be leveraged to boost the hydrolytic activity of Zr₆ MOF nanozymes. Presumably, a future improved synthesis of a more defective variant of UiO-66-NO₂ should result in an even higher proteolytic activity.⁵⁰

Effect of synthesis modulator. The results discussed above prompted us to complement our evaluation of structural changes by inducing defects in the standard UiO-66 and evaluating its hydrolytic activity in the same conditions. To induce the formation of defects in the standard UiO-66 structure (hereon, UiO-66-TFA), we synthesized it in the presence of trifluoroacetic acid (TFA), which is effective in inducing ‘missing linkers’ defects and exposing more coordinatively unsaturated Zr sites (PXRD in Figure S3).⁴¹ As expected, a high surface area (985 m²/g) and a low linker/node ratio (Linkers coord./Zr₆ cluster = 7) were obtained from N₂ physisorption isotherm and TGA measurements (Figure S1 and S2), while the particle size remained similar to the other UiO-66 MOFs prepared before (Figure 3). Not surprisingly, the hydrolysis of Gly-Gly under standard conditions (Scheme 1b) proceeded with a rate constant $79.7 \times 10^{-7} \text{ s}^{-1}$ ($t_{1/2} = 24.2 \text{ h}$) (Figure S7). This reaction rate is similar to the ones obtained for UiO-66-NH₂/NO₂. Such similarity further confirms the strong boosting effect of defects in the hydrolytic activity of UiO-66 towards the peptide bond. While above it was demonstrated that defects could overcome the electronic deactivation of an electron-donating linker (UiO-66-NH₂), the similar reactivity of UiO-66-TFA suggests that a higher Lewis acidity induced by an electron-withdrawing linker can be mimicked by a more defective structure. Such scenario points again to the cumulative boosting effect that can be expected by combining electron-withdrawing linkers with a defective structure.

Insights in the nature of catalytic site of UiO-66 analogues

The results discussed above underline the advantages for the hydrolysis of peptide bonds by enhancing the Lewis acidity of the Zr₆ node through the use of electron-withdrawing ligands or by increasing the number of defects. However, the three modified MOFs may likely have distinctive catalytic sites, which may further impact their reactivity. To this end, we compared UiO-66-NH₂, UiO-66-NO₂ and UiO-66-TFA reactivity i) under different pD conditions, ii) in the presence of inhibitors and iii) toward the hydrolysis of several Gly-X dipeptides (X = amino acid). Given the inherent adsorption capacity of MOFs, we started our comparison by probing the adsorption of Gly-Gly in these MOFs since UiO-66-NO₂/NH₂ are more likely to engage in hydrogen bonding interactions with the substrate when compared to MOF-808 which was previously also shown to exhibit peptidase activity.¹² As expected, UiO-66-NO₂/NH₂ showed a greater adsorption capacity in comparison with the parent UiO-66 structure, probably due to the H-bonding capability of these

residues. However, the low adsorption capacity of UiO-66-TFA seems to indicate that adsorption and reactivity are not necessarily directly correlated in this case (Figure S15 and S16).

All UiO-66 analogues presented a similar reaction profile when different pD conditions or inhibitors were used. The hydrolytic activity of UiO-66-NH₂, UiO-66-NO₂ and UiO-66-TFA towards Gly-Gly topped around pD 8.0 when the pD of the reaction was varied from 4.2 to 9.5 (Figure S17), which generally coincides with the stability threshold of these MOFs in alkaline medium (Figure S18). Likewise, marked inhibition of the hydrolysis reaction was observed across the board in the presence of several nonreactive bis-carboxylic acids inhibitors (Figure 4), with a slightly better performance observed for the UiO-66-NH₂. Curiously, smaller diacids like malonic, malic, citric acid and oxalic acids affected the overall activity more than larger inhibitors like succinic, glutaric and adipic acids. The correlation between reaction inhibition and size of the diacid inhibitor is different than the strong inhibition observed with MOF-808, suggesting that the UiO-66 is less prone to strongly bind larger molecules.¹² Moreover, the significantly better performance of UiO-66-NH₂ in comparison to UiO-66-NO₂/TFA in the presence of adipic acid (1) raises the possibility of a favorable linker-inhibitor interaction that could prevent the diacid to block the active Zr site.^{46, 49}

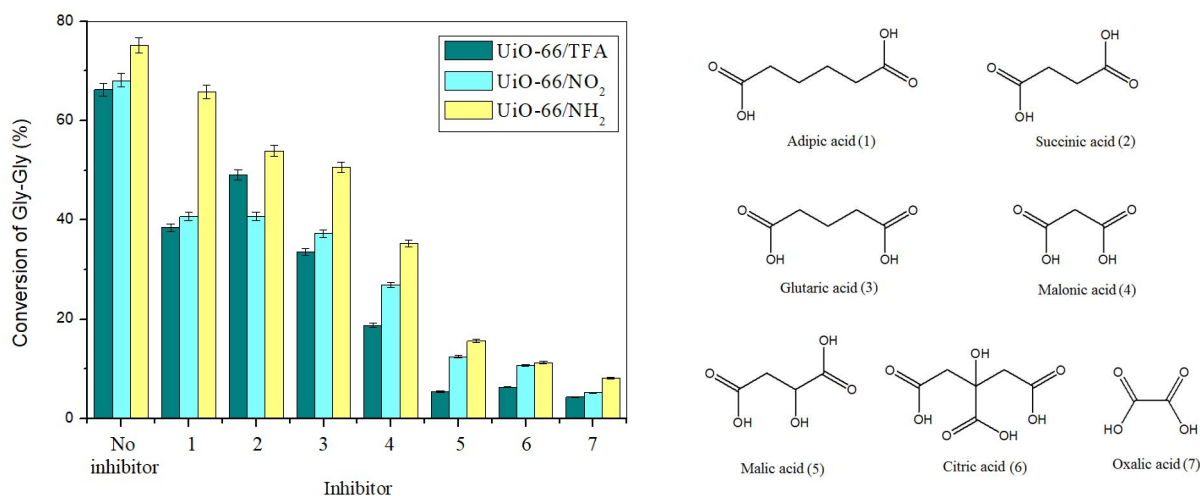


Figure 4. Smaller dicarboxylic acids were more efficient inhibitors of Gly-Gly hydrolysis by UiO-66 analogues. *Conditions:* 2.0 μmol of Gly-Gly, 2.0 μmol of the studied MOF, and 5.0 μmol of the inhibitor after 2 days at pD 7.8 and 60 °C.

Although UiO-66-NH₂, UiO-66-NO₂ and UiO-66-TFA responded similarly to changes in the reaction conditions, interesting differences were observed when a series of 15 Gly-X dipeptides (X = amino acid) were examined as substrates (Figure 5). In general, the hydrolysis efficiency decreased upon increasing the steric hindrance of X side chain, as evidenced by the lower conversions observed upon increase of Gly-X volume regardless of the nature of their functional group. In addition, for all three MOFs very similar reactivities were observed when X = Val, Leu

and Ile, which are residues that can impart various degrees of steric hindrance. This indicates minimal steric influence of NO₂ and NH₂ groups on UiO-66-NO₂/NH₂ catalytic activity, suggesting that the differences observed among Gly-X series derive from other structural or electronic features. On the other hand, the Gly-X dipeptides hydrolyzed more efficiently were different for each UiO-66 analog. UiO-66-TFA showed a marked preference for the hydrolysis of dipeptides containing nucleophilic groups that can undergo an intramolecular *N,O*-rearrangement such as Gly-Ser and Gly-Asp. This rearrangement generates an intermediate ester, which is then quickly hydrolyzed. Considering the hydrolysis of proteins in acidic medium reported previously, such trend suggests a greater contribution of Brønsted acidity in these reactions.⁵¹ Moreover, the surface acidity of group IV metal-oxo clusters has previously favored the cleavage of Asp-X/X-Asp in horse-heart myoglobin.¹⁴ On the other hand, a more homogeneous distribution of Gly-X conversion rates observed for UiO-66-NH₂/NO₂, with a greater effect observed for the more electron-poor UiO-66-NO₂, pointed to a greater contribution of a standard Lewis acid activation of the amide group, since substrates like Gly-Ser/Asp peptides did not present an increased reactivity compared to other substrates.¹⁶

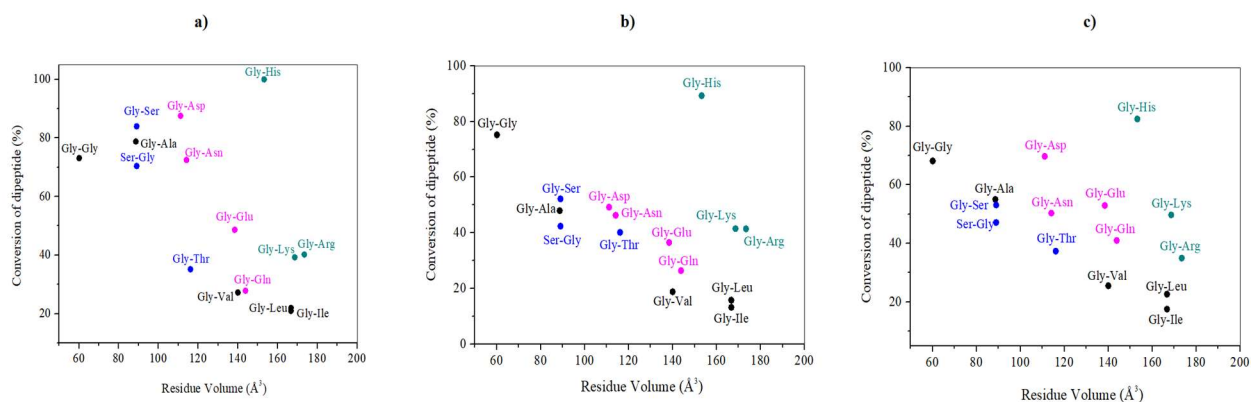


Figure 5. Conversion of dipeptides after (a) 3 days in the presence of UiO-66-TFA, (b) 2 days in the presence of UiO-66-NH₂ and (c) 2 days in the presence of UiO-66-NO₂ as a function of the volume of amino acid X (2.0 μmol of Gly-X dipeptides + 2.0 μmol of MOF, pD 7.8 and 60 °C).

Together, these results indicate that besides improved reactivity, different selectivity in the peptide bond cleavage can likely be achieved using different strategies to manipulate the structure around the catalytic site. Further, such selectivity might derive not only from distinct coordination preferences of each substrate but also from fine tuning the Brønsted and Lewis acid contributions in the hydrolysis pathway.⁵² These trends become even more interesting when we take into consideration the strikingly similar experimental activation parameters for three UiO-66 analogues obtained through the Arrhenius and Eyring equations using reaction kinetic data of experiments carried out at different temperatures (Table 2, and Figures S19-S22). Consistent with the reaction rate constants reported above, this similarity indicates the reactivity is equally improved in all three

UiO-66 analogs, even though the contributions of Brønsted and Lewis acid pathways to the overall hydrolysis reaction likely vary between the structures. Excitingly, this suggests that selectivity (i.e., mechanism of hydrolysis) and catalytic activity could be tuned independently from each other.

Table 2. Experimental activation parameters of the hydrolysis of Gly-Gly by UiO-66 MOFs at pD 7.8.

MOF	E_a (kJ mol ⁻¹)	ΔH^\ddagger (kJ mol ⁻¹)	ΔS^\ddagger (J mol ⁻¹ K ⁻¹)	ΔG^\ddagger at 310 K (kJ mol ⁻¹)
UiO-66-NH ₂	79 ± 1	76 ± 1	- 112 ± 1	111 ± 1
UiO-66-NO ₂	82 ± 1	79 ± 1	- 105 ± 1	111 ± 1
UiO-66-TFA	78 ± 1	75 ± 1	- 117 ± 1	112 ± 1

CONCLUSION

In summary, the strategies to modify the structure of Zr-based MOFs by modulating the linker electronics or increasing the number of defects resulted in significant increase in the reaction rates of UiO-66 mediated peptide hydrolysis. While standard UiO-66 successfully showcased the potential of UiO-66 as a heterogeneous artificial nanoprotease, modified derivatives, which conserved crystallinity and particle sized but provided a distinct nanopore environment, clearly presented a more attractive reactivity profile. Surprisingly, the catalytic activity of UiO-66-NH₂ derivative is higher than expected considering solely linker electronics influence on the Zr₆-node, suggesting that defect sites play a prominent role in promoting reactivity by both increasing the number of catalytic sites available and streamlining the access of substrates to these sites due to the larger nanopores present. These observations were ratified by the similar reactivity observed for UiO-66-TFA. On the other hand, the least defective UiO-66-NO₂, which also presented the lowest surface area and kept the nanopore size distribution rather similar to the parent UiO-66 MOF, was as active as the other analogues, indicating that increasing the Lewis acidity is also an effective strategy to increase reactivity. Apart from the boost in reactivity, UiO-66 analogues provided distinct reactivity patterns towards a series of Gly-X dipeptides, thereby highlighting the potential of developing residue-selective artificial peptidases. Initial analysis of this pattern revealed a marked but general effect of the substrate size, suggesting that changes imparted in the nanoporous network were not responsible for the different reactivity. On the other side, the results suggest that distinct Brønsted and Lewis acid contributions to the hydrolytic reaction pathway might be at the origin of the different reactivities observed. Further studies exploiting these structural changes in the design of other heterogeneous nanozymes with improved proteolytic activity are ongoing in our lab and will be published in due course.

ASSOCIATED CONTENT

Supporting Information Experimental procedures, MOF characterization, supplementary data for peptide and protein hydrolysis experiments.

AUTHOR INFORMATION

Corresponding Author

*tatjana.vogt@kuleuven.be

ORCID

Hong Giang T. Ly: orcid.org/0000-0003-4783-7417

Guangxia Fu: orcid.org/0000-0002-9909-3985

Francisco de Azambuja: orcid.org/0000-0002-5537-5411

Dirk De Vos: orcid.org/0000-0003-0490-9652

Tatjana N. Parac-Vogt: orcid.org/0000-0002-6188-3957

Notes

The authors declare no competing financial interest.

ACKNOWLEDGEMENTS

H.G.T.L. thanks the FWO (Research Foundation – Flanders) for the postdoctoral fellowship. G. F. thanks the CSC for fellowship (grant number: 201406230044). F.d.A. thanks KU Leuven for the postdoctoral fellowship. T.N.P.V and D.D.V. thank FWO for the financial support under project G095017N. T.N.P.V thanks the European Commission for the funding under the Horizon 2020, FoodEnTwin project, GA No. 810752.

REFERENCES

1. Bakhtiar, R.; Thomas, J. J.; Siuzdak, G., Mass Spectrometry in Viral Proteomics. *Acc. Chem. Res.* **2000**, *33* (3), 179-187.
2. Muir, T. W., Semisynthesis of Proteins by Expressed Protein Ligation. *Annu. Rev. Biochem* **2003**, *72* (1), 249-289.
3. Durek, T.; Becker, C. F. W., Protein semi-synthesis: New proteins for functional and structural studies. *Biomol. Eng* **2005**, *22* (5), 153-172.
4. Westermeier, R.; Naven, T., Proteomics in Practice: A Laboratory Manual of Proteome Analysis. 3rd ed.; Wiley-VCH Verlag GmbH: 2002.
5. Rodriguez, J.; Gupta, N.; Smith, R. D.; Pevzner, P. A., Does Trypsin Cut Before Proline? *Journal of Proteome Research* **2008**, *7* (1), 300-305.

6. Swaney, D. L.; Wenger, C. D.; Coon, J. J., Value of Using Multiple Proteases for Large-Scale Mass Spectrometry-Based Proteomics. *Journal of Proteome Research* **2010**, *9* (3), 1323-1329.
7. Tsiatsiani, L.; Heck, A. J. R., Proteomics beyond trypsin. *The FEBS Journal* **2015**, *282* (14), 2612-2626.
8. Wei, H.; Wang, E., Nanomaterials with enzyme-like characteristics (nanozymes): next-generation artificial enzymes. *Chem. Soc. Rev.* **2013**, *42* (14), 6060-6093.
9. Huang, Y.; Ren, J.; Qu, X., Nanozymes: Classification, Catalytic Mechanisms, Activity Regulation, and Applications. *Chem. Rev.* **2019**, *119* (6), 4357-4412.
10. Wu, J.; Wang, X.; Wang, Q.; Lou, Z.; Li, S.; Zhu, Y.; Qin, L.; Wei, H., Nanomaterials with enzyme-like characteristics (nanozymes): next-generation artificial enzymes (II). *Chem. Soc. Rev.* **2019**, *48* (4), 1004-1076.
11. Li, B.; Chen, D.; Wang, J.; Yan, Z.; Jiang, L.; Deliang, D.; He, J.; Luo, Z.; Zhang, J.; Yuan, F., MOFzyme: Intrinsic protease-like activity of Cu-MOF. *Scientific Reports* **2014**, *4*, 6759.
12. Ly, H. G. T.; Fu, G.; Kondinski, A.; Bueken, B.; De Vos, D.; Parac-Vogt, T. N., Superactivity of MOF-808 toward Peptide Bond Hydrolysis. *J. Am. Chem. Soc.* **2018**, *140* (20), 6325-6335.
13. Loosen, A.; de Azambuja, F.; Smolders, S.; Moons, J.; Simms, C.; De Vos, D.; Parac-Vogt, T. N., Interplay between structural parameters and reactivity of Zr₆-based MOFs as artificial proteases. *Chem. Sci.* **2020**, *11* (26), 6662-6669.
14. Moons, J.; de Azambuja, F.; Mihailovic, J.; Kozma, K.; Smiljanic, K.; Amiri, M.; Cirkovic Velickovic, T.; Nyman, M.; Parac-Vogt, T. N., Discrete Hf₁₈ Metal-oxo Cluster as a Heterogeneous Nanozyme for Site-Specific Proteolysis. *Angew. Chem. Int. Ed.* **2020**, *59* (23), 9094-9101.
15. Kathryn, B. G.; Miki, K., Major Advances in the Hydrolysis of Peptides and Proteins by Metal Ions and Complexes. *Curr. Org. Chem.* **2006**, *10* (9), 1035-1049.
16. Wezynfeld, N. E.; Frączyk, T.; Bal, W., Metal assisted peptide bond hydrolysis: Chemistry, biotechnology and toxicological implications. *Coord. Chem. Rev.* **2016**, *327-328*, 166-187.
17. Absillis, G.; Parac-Vogt, T. N., Peptide Bond Hydrolysis Catalyzed by the Wells–Dawson Zr(α_2 -P₂W₁₇O₆₁)₂ Polyoxometalate. *Inorg. Chem.* **2012**, *51* (18), 9902-9910.
18. Ly, H. G. T.; Absillis, G.; Parac-Vogt, T. N., Amide bond hydrolysis in peptides and cyclic peptides catalyzed by a dimeric Zr(IV)-substituted Keggin type polyoxometalate. *Dalton Trans.* **2013**, *42* (30), 10929-10938.
19. Vanhaecht, S.; Absillis, G.; Parac-Vogt, T. N., Amino acid side chain induced selectivity in the hydrolysis of peptides catalyzed by a Zr(IV)-substituted Wells-Dawson type polyoxometalate. *Dalton Trans.* **2013**, *42* (43), 15437-15446.
20. Ly, H. G. T.; Absillis, G.; Parac-Vogt, T. N., Comparative Study of the Reactivity of Zirconium(IV)-Substituted Polyoxometalates towards the Hydrolysis of Oligopeptides. *Eur. J. Inorg. Chem.* **2015**, *2015* (13), 2206-2215.
21. Ly, H. G. T.; Mihaylov, T.; Absillis, G.; Pierloot, K.; Parac-Vogt, T. N., Reactivity of Dimeric Tetrazirconium(IV) Wells–Dawson Polyoxometalate toward Dipeptide Hydrolysis Studied by a Combined Experimental and Density Functional Theory Approach. *Inorg. Chem.* **2015**, *54* (23), 11477-11492.

22. Stroobants, K.; Moelants, E.; Ly, H. G. T.; Proost, P.; Bartik, K.; Parac-Vogt, T. N., Polyoxometalates as a Novel Class of Artificial Proteases: Selective Hydrolysis of Lysozyme under Physiological pH and Temperature Promoted by a Cerium(IV) Keggin-Type Polyoxometalate. *Chem. Eur. J* **2013**, *19* (8), 2848-2858.
23. Stroobants, K.; Absillis, G.; Moelants, E.; Proost, P.; Parac-Vogt, T. N., Regioselective Hydrolysis of Human Serum Albumin by Zr-IV-Substituted Polyoxotungstates at the Interface of Positively Charged Protein Surface Patches and Negatively Charged Amino Acid Residues. *Chem. Eur. J* **2014**, *20* (14), 3894-3897.
24. Stroobants, K.; Ho, P. H.; Moelants, E.; Proost, P.; Parac-Vogt, T. N., Selective hydrolysis of hen egg white lysozyme at Asp-X peptide bonds promoted by oxomolybdate. *J. Inorg. Biochem.* **2014**, *136*, 73-80.
25. Sap, A.; Absillis, G.; Parac-Vogt, T. N., Selective hydrolysis of oxidized insulin chain B by a Zr(IV)-substituted Wells-Dawson polyoxometalate. *Dalton Trans.* **2015**, *44* (4), 1539-1548.
26. Sap, A.; De Zitter, E.; Van Meervelt, L.; Parac-Vogt, T. N., Structural Characterization of the Complex between Hen Egg-White Lysozyme and ZrIV-Substituted Keggin Polyoxometalate as Artificial Protease. *Chem. Eur. J.* **2015**, *21* (33), 11692-11695.
27. Ly, H. G. T.; Absillis, G.; Janssens, R.; Proost, P.; Parac-Vogt, T. N., Highly Amino Acid Selective Hydrolysis of Myoglobin at Aspartate Residues as Promoted by Zirconium(IV)-Substituted Polyoxometalates. *Angew. Chem., Int. Ed.* **2015**, *54* (25), 7391-7394.
28. Vandebroek, L.; De Zitter, E.; Ly, H. G. T.; Conić, D.; Mihaylov, T.; Sap, A.; Proost, P.; Pierloot, K.; Van Meervelt, L.; Parac-Vogt, T. N., Protein-Assisted Formation and Stabilization of Catalytically Active Polyoxometalate Species. *Chem. Eur. J.* **2018**, *24* (40), 10099-10108.
29. Ly, H. G. T.; Mihaylov, T. T.; Proost, P.; Pierloot, K.; Harvey, J. N.; Parac-Vogt, T. N., Chemical Mimics of Aspartate-Directed Proteases: Predictive and Strictly Specific Hydrolysis of a Globular Protein at Asp-X Sequence Promoted by Polyoxometalate Complexes Rationalized by a Combined Experimental and Theoretical Approach. *Chem. Eur. J.* **2019**, *25* (63), 14370-14381.
30. Diercks, C. S.; Kalmutzki, M. J.; Diercks, N. J.; Yaghi, O. M., Conceptual Advances from Werner Complexes to Metal-Organic Frameworks. *ACS Cent. Sci.* **2018**, *4* (11), 1457-1464.
31. Lu, W. G.; Wei, Z. W.; Gu, Z. Y.; Liu, T. F.; Park, J.; Tian, J.; Zhang, M. W.; Zhang, Q.; Gentle, T.; Bosch, M.; Zhou, H. C., Tuning the structure and function of metal-organic frameworks via linker design. *Chem. Soc. Rev.* **2014**, *43* (16), 5561-5593.
32. Li, J.-R.; Kuppler, R. J.; Zhou, H.-C., Selective gas adsorption and separation in metal-organic frameworks. *Chem. Soc. Rev.* **2009**, *38* (5), 1477-1504.
33. Plonka, A. M.; Wang, Q.; Gordon, W. O.; Balboa, A.; Troya, D.; Guo, W.; Sharp, C. H.; Senanayake, S. D.; Morris, J. R.; Hill, C. L.; Frenkel, A. I., In Situ Probes of Capture and Decomposition of Chemical Warfare Agent Simulants by Zr-Based Metal Organic Frameworks. *J. Am. Chem. Soc.* **2017**, *139* (2), 599-602.
34. Horcajada, P.; Gref, R.; Baati, T.; Allan, P. K.; Maurin, G.; Couvreur, P.; Férey, G.; Morris, R. E.; Serre, C., Metal-Organic Frameworks in Biomedicine. *Chem. Rev.* **2012**, *112* (2), 1232-1268.
35. Bour, J.; Wright, A. M.; He, X.; Dinca, M., Bioinspired Chemistry at MOF Secondary Building Units. *Chem. Sci.* **2020**, *11* (7), 1728-1737.

36. Rogge, S. M. J.; Bavykina, A.; Hajek, J.; Garcia, H.; Olivos-Suarez, A. I.; Sepúlveda-Escribano, A.; Vimont, A.; Clet, G.; Bazin, P.; Kapteijn, F.; Daturi, M.; Ramos-Fernandez, E. V.; Llabrés i Xamena, F. X.; Van Speybroeck, V.; Gascon, J., Metal-organic and covalent organic frameworks as single-site catalysts. *Chem. Soc. Rev.* **2017**, *46* (11), 3134-3184.
37. Dhakshinamoorthy, A.; Li, Z.; Garcia, H., Catalysis and photocatalysis by metal organic frameworks. *Chem. Soc. Rev.* **2018**, *47* (22), 8134-8172.
38. Pascanu, V.; González Miera, G.; Inge, A. K.; Martín-Matute, B., Metal-Organic Frameworks as Catalysts for Organic Synthesis: A Critical Perspective. *J. Am. Chem. Soc.* **2019**, *141* (18), 7223-7234.
39. Winarta, J.; Shan, B.; McIntyre, S. M.; Ye, L.; Wang, C.; Liu, J.; Mu, B., A Decade of UiO-66 Research: A Historic Review of Dynamic Structure, Synthesis Mechanisms, and Characterization Techniques of an Archetypal Metal-Organic Framework. *Cryst. Growth Des.* **2020**, *20* (2), 1347-1362.
40. Vermoortele, F.; Vandichel, M.; Van de Voorde, B.; Ameloot, R.; Waroquier, M.; Van Speybroeck, V.; De Vos, D. E., Electronic Effects of Linker Substitution on Lewis Acid Catalysis with Metal-Organic Frameworks. *Angew. Chem. Int. Ed.* **2012**, *51* (20), 4887-4890.
41. Vermoortele, F.; Bueken, B.; Le Bars, G.; Van de Voorde, B.; Vandichel, M.; Houthoofd, K.; Vimont, A.; Daturi, M.; Waroquier, M.; Van Speybroeck, V.; Kirschhock, C.; De Vos, D. E., Synthesis Modulation as a Tool To Increase the Catalytic Activity of Metal-Organic Frameworks: The Unique Case of UiO-66(Zr). *J. Am. Chem. Soc.* **2013**, *135* (31), 11465-11468.
42. Fang, Z.; Bueken, B.; De Vos, D. E.; Fischer, R. A., Defect-Engineered Metal-Organic Frameworks. *Angew. Chem. Int. Ed.* **2015**, *54* (25), 7234-7254.
43. Loosen, A.; de Azambuja, F.; Smolders, S.; Moons, J.; Simms, C.; De Vos, D. E.; Parac-Vogt, T., Interplay between structural parameters and reactivity of Zr₆-based MOFs as artificial proteases. *Chem. Sci.* **2020**, DOI: 10.1039/D0SC02136A.
44. Radzicka, A.; Wolfenden, R., Rates of Uncatalyzed Peptide Bond Hydrolysis in Neutral Solution and the Transition State Affinities of Proteases. *J. Am. Chem. Soc.* **1996**, *118* (26), 6105-6109.
45. Katz, M. J.; Brown, Z. J.; Colón, Y. J.; Siu, P. W.; Scheidt, K. A.; Snurr, R. Q.; Hupp, J. T.; Farha, O. K., A facile synthesis of UiO-66, UiO-67 and their derivatives. *Chem. Commun.* **2013**, *49* (82), 9449-9451.
46. Fu, G.; Cirujano, F. G.; Krajnc, A.; Mali, G.; Henrion, M.; Smolders, S.; De Vos, D. E., Unexpected linker-dependent Brønsted acidity in the (Zr)UiO-66 metal organic framework and application to biomass valorization. *Catal. Sci. Technol.* **2020**, *10* (12), 4002-4009.
47. Valenzano, L.; Civalleri, B.; Chavan, S.; Bordiga, S.; Nilsen, M. H.; Jakobsen, S.; Lillerud, K. P.; Lamberti, C., Disclosing the Complex Structure of UiO-66 Metal Organic Framework: A Synergic Combination of Experiment and Theory. *Chem. Mater.* **2011**, *23* (7), 1700-1718.
48. Shan, B.; McIntyre, S. M.; Armstrong, M. R.; Shen, Y.; Mu, B., Investigation of Missing-Cluster Defects in UiO-66 and Ferrocene Deposition into Defect-Induced Cavities. *Ind. Eng. Chem. Res.* **2018**, *57* (42), 14233-14241.
49. Hajek, J.; Vandichel, M.; Van de Voorde, B.; Bueken, B.; De Vos, D.; Waroquier, M.; Van Speybroeck, V., Mechanistic studies of aldol condensations in UiO-66 and UiO-66-NH₂ metal organic frameworks. *J. Catal.* **2015**, *331*, 1-12.

50. Feng, X.; Hajek, J.; Jena, H. S.; Wang, G.; Veerapandian, S. K. P.; Morent, R.; De Geyter, N.; Leysens, K.; Hoffman, A. E. J.; Meynen, V.; Marquez, C.; De Vos, D. E.; Van Speybroeck, V.; Leus, K.; Van Der Voort, P., Engineering a Highly Defective Stable UiO-66 with Tunable Lewis- Brønsted Acidity: The Role of the Hemilabile Linker. *J. Am. Chem. Soc.* **2020**, *142* (6), 3174-3183.
51. Oliyai, C.; Borchardt, R. T., Chemical Pathways of Peptide Degradation. IV. Pathways, Kinetics, and Mechanism of Degradation of an Aspartyl Residue in a Model Hexapeptide. *Pharm. Res.* **1993**, *10* (1), 95-102.
52. Cirujano, F. G.; Llabrés i Xamena, F. X., Tuning the Catalytic Properties of UiO-66 Metal–Organic Frameworks: From Lewis to Defect-Induced Brønsted Acidity. *The Journal of Physical Chemistry Letters* **2020**, *11* (12), 4879-4890.

Table of Contents graphic:

